# Shaft stability assessment with numerical simulation

Dinis Mário Miranda
dinis.miranda@tecnico.ulisboa.pt

Instituto Superior Técnico, Lisboa, Portugal

September 2020

**Abstract**

Ventilation is essential in mining exploitation to provide oxygen and ensure the quality of air necessary to breathe, to dilute and remove nocive gases from equipment and blasts, to reduce the natural temperature of the rocks and much more, for this reason, it becomes more and more important to ensure the operationality of the ventilation shaft during the exploitation. Stability analysis is so important to design and definite strategy to open the shaft. According to this, the main focus of this master thesis is to analyze the stability of $10$ ventilation shafts of Neves-Corvo mine, from $300m$ to $800m$ depth between two underground levels.

For this purpose, we used the McCracken and Stacey(MS) method to predict the stability of the ventilation shaft using geomechanical classifications, and then, was used $3D$ Rocscience numerical modeling software $RS^3$ to analyze the stability due to the field stress.

The results obtained in this analysis allowed to identify potential instable zones and conclude that $50\%$ of the selected ventilation shafts have stability problems due to the field stress variation, originating wide breakout/dog-ear breakout, that coincide with $90\%$ with in situ classifcation; as for the MS, only $20\%$ was classified as potentially unstable, which corresponds to $60\%$ with reality.
**Keywords:** Ventilation shaft; Raise Bore; Stability; Numerical Modelling.

## 1. Introduction

From the most remote times of civilization to the present day, man uses mining techniques to explore minerals close to the earth's surface to manufacture weapons and tools [1]. As time goes by, resources at the surface are exhausted, which forces man to search in greater depths, thus making the exploration process complex and challenging.

Mining is one of the oldest activities developed by man along with agriculture. In the beginning, miners used primitive tools to excavate making the exploitation process complex and slow [1]. The acquired experience and technological advances allow exploiting high depth, making the solution essential and complex in underground exploitations due to the presence of harmful gases, dust, lack of oxygen and high prices [2].

For air intake and exhaust in the high depths stoping are used ventilation shaft [3] Shaft used for air intake or exhaust must last as long as possible at least as long as the exploitation lasts, owing to is used to decrease the temperature, as well as remove and dilute undesirable gases and dusts [2].

Technological advances and digital transformation allow the man to create more and more complex models to understand the world in order to help in decision making. Computational models are essential to analyze and explain natural phenomena, which is why they are increasingly used in several areas of Engineering. In this work, numerical modeling will be used to assess the shaft stability.

Throughout this dissertation, the geomechanical classification method applied to the shaft will be presented and, the concepts related to the stress distribution around them using numerical modeling in order to predict the damage, thus avoiding eventual rehabilitation or collapse, which reduces significantly the costs.

This dissertation has as an objective to introduce into the shaft stability assessment model, field stress variation due to geometry using numerical modeling, in order to identify potentially unstable zones not describe in the traditional method carried out using geomechanical classifications.

## 2. Background

### 2.1. Shaft

In the mining industry, the shafts are the vertical or sub-vertical excavation developed to connect two levels of underground mining[4].

The shafts can be classified according to their function, such as: ventilation shaft, ore shaft(ore passes), hoisting shaft.

The ventilation shaft are built with the purpose of allowing air to pass between two levels of the mine

[4]. They can be classified as: air intake, when they allow clean air to through from the upper level to a lower level in the mine, and exhaust, when they allow contaminated air to through from lower levels to the upper levels.

Ore passes are used to through the ore from a higher level to lower levels [4]. This type of shaft is only built between two levels in depth and never from the surface.

Hoisting shaft is the infrastructure used to remove material produced in the mine, which may be ore or waste. This type of shaft is just built from the surface to a low horizontal level designed to hoist material.

In the hoisting shaft the material produced from the blasts is transported to the surface by skips, and can be equipped with cages skip where workers, equipment and materials are transported to the mine. In addition to transporting the material, this infrastructure also serves for fresh air to enter the mine and the passage of electricity cables and/or water pipes can be used [4].

Shaft opening is a complex, delicate and time-consuming operation. Therefore, it must be properly planned in order to avoid accidents, high costs and delays in the project. To open a shaft, two main techniques are used [5]: shaft sinking and raise boring.

Shaft sinking: is an opening technique shafts from top to bottom with the use of explosives. This technique doesn't require access to the base [6].

Raise boring: is an opening technique shaft from the bottom to top, using drilling equipment (raise bore [1] machine), access to the bottom not required [6].

After opening the shaft, the main concern is the stability of the surrounding rock mass. The raise bore technique minimizes disturbances to the rock surrounding the shaft [5], for this reason is the most used worldwide technique[6], Its advantages over the conventional shaft sinking are: safety, because no one works inside the shaft; minimizes the damage surrounding rock; softens the shaft walls, thus minimize resistance to air circulation; continuous and faster process; reduced labor and lower operating costs.

The stability of underground excavations depends on the strength of the rock mass around the excavation and on the induced stress [7]. As in other types of underground excavation, several geological and geotechnical factors affect shaft stability [6], such as: lithology; weathering; main structural characteristics: faults, folds, wall and ceiling contacts, etc; groundwater; stress in situ and change in the field stress over time.

[1] Drilling equipment used in underground mines to develop vertical holes between two levels without explosives.

Shaft instability is caused by a combination of several factors. These factors can be classified as controllable and uncontrollable[8].

The controllable factors are the factors that man can control, are related to the geometric characteristics of the shaft and to the drilling operation. Uncontrollable factors are characteristic of geological formations and therefore the man is unable to change, they are related to the physical, chemical and geomechanical properties of rocks[8].

### 2.2. Stability assessment of underground excavations

Rock masses stability analysis is done through the properties identified by laboratory tests or in situ tests, however, laboratory tests do not provide realistic properties of resistance, deformation and behavior of fractures in the rock mass [9]. While the in situ tests show better results, but they are difficult to perform because they need more time to be done, they have high costs and it is difficult to control the initial conditions [9].

The most applied methods for stability assessment can be classified as follows [10] [9]:

- Empirical methods;
- Numerical methods;
- Data Mining.

#### 2.2.1 Empirical methods

Geomechanical classification methods are good examples of empirical methods, these are derived from engineering experiences acquired in previous projects [9].

There are several empirical methods developed by different authors to classify rock masses. However, methods applied to stability shaft analysis are: RQD, Q-system, Raise bore quality ($Q_r$)

RQD classification is the percentage of fragments recovered from drilling to provide an estimate of the quality of the rock mass relative to the total length of the drilling and can be determined by equation 1 [11]. See table 1.

$$RQD = \frac{\sum_{i=1}^{n} l_i}{L} \times 100 \quad (1)$$

Wherein the respective parameters have the following meanings: $RQD$ is the rock quality designation; $l_i$ is the length of fragments over $100mm$ and $L$ the total length

**Table 1:** RQD Classification [11]

| **RQD** | **0-25** | **25-50** | **50-75** | **75-90** | **90-100** |
|---|---|---|---|---|---|
| **Quality** | Very poor | Poor | Fair | Good | Excellent |

The Q-System classification is also known as Barton's classification in honor of Nick Ryland Barton. This classification is used to qualitatively estimate stoping and tunnel supports based on the rock quality assessment [12]. The Q-System classification can be determined by equation 2.

$$Q = \left(\frac{RQD}{J_n}\right) \times \left(\frac{J_r}{J_a}\right) \times \left(\frac{J_w}{SRF}\right) \quad (2)$$

Wherein $RQD$ is the rock quality designation, $J_n$ is joint set number, $J_r$ is joint roughness number, $J_a$ is the joint alteration number, $J_w$ is joint water factor and $SRF$ is the stress reduction factor

Raise bore quality index, $Q_r$, is the method used for shaft stability analysis proposed by McCracken & Stacey $(MS)$, and is also considered as adjusted Q-system. The adjustment factors are: the walls because they control the final stability owing to the fact that there is no roof in excavation; the orientation and weathering of the rock [5]. Raise bore quality, $Q_r$ is determined by equation 3.

$$Q_r = Q_{sidewall} \times Q \times O \times W \quad (3)$$

where $Q_{sidewall}$ represents the adjustment factor due to the shaft walls, $O$, adjustment factor due to orientation adjustment , $W$, weathering adjustment.

Barton classification, is mainly concerned about roof stability of the excavation, whereas in the shaft the major concern is on the walls, therefore, McCracken & Stacey due to the experiments done in previous projects propose adjustments factor to be applied on Q-system called $Q_{sidewall}$ as indicated in (4) [5]:

$$Q_{sidewall} = 2,5 \quad \text{if } Q > 1 \quad 1 \quad \text{if } Q \leq 1 \quad (4)$$

The orientation adjustment factor proposed by McCracken & Stacey is ilustrated in the table 2.

**Table 2:** McCracken and Stacey orientation adjustment factors[5]

| Nº of major joint sets | **Flat (0-30°)** | **Steep (60-90°)** |
|---|---|---|
| **1** | $0,85$ | $0,85$ |
| **2** | $0,75$ | $0,75$ |
| **3** | $0,60$ | $0,60$ |

The adjustments due to rock weathering $(W)$ proposed by $MS$ for the $Q$ parameter are: $0.9; 0.75$ or $0.5$ for light, moderate and severe weathering of intact rock walls [5].

The quality index of the raise bore, $Q_r$, is not sufficient to determine the shaft stability, because for the same quality of the rock mass, different results are obtained depending on the span created by the shaft. For this reason, stability can be determined in terms of the maximum span without support using the equation 5 [5]:

$$Span_{Max} = 2 \times RSR \times Q_R^{0,4} \quad (5)$$

Where $RSR$ is raise stability ratio ($RSR = 1.3$ for ventilation shaft and $RSR = 1.6$ for ore passes) and $Q_R$ is the raise bore quality.

### 2.2.2 Numerical methods

The advancement of technology has helped man to describe and understand the behavior of the rock mass around the excavations, during and after opening, in order to predict and solve problems related to stability.

Nowadays, tools that use advanced numerical methods have become an important part in engineering projects development phase. These tools are useful to simulate rock mass behavior, stress distribution, safety factor and displacements [13].

There are several methods and softwares for numerical analysis used according to the conditions to simulate the rock mass behavior arround the excavation [13]. Numerical methods can be classified as follows [14]

- Continuous methods: finite difference method (FDM), finite element method (FEM), and boundary element method (BEM);
- Discontinuous methods: discrete element methods (DEM), discrete fracture network methods (DFNM);
- Hybrid method.

Continuous methods are more used than the discontinuous, due to the fact that the computational requirements are simple, and parameters needed for the analysis are easier to obtain from evaluations in situ and in the laboratory [14]. The main differences between this two methods are the ability to rotate and detach the blocks in the deformation process, and only discontinuous method allows to perform this rotation; while the hybrid method is a combination of continuous and descontinuous methods [14].

In the scope of this work, analysis of underground excavations, it has opted the rocscience software, specifically $RS^3$, considering the vast package they offer to the mining industries and the availability in IST mine laboratories. $RS^3$ uses the finite element method to solve the proposed problems [15].

The basis of the finite element method, consists of dividing the geometry of the complex problem around the excavation, into small ones in interconnected elements in order to subdivide into simpler problems.

The elements can have different geometries depending on the problem, such as triangular, quadrilateral and others. The connection between the elements is made through nodes, and the set of all elements and nodes are called mesh.

### 2.2.3 Data Mining

Data mining is one of the advanced analytical solutions, and it is emerging every time with the increasing amount of data. This technique is recent and goes beyond statistics, being also concerned with pattern recognition, and automatic search for solutions from a vast set of data[16].

According to McCarthy, artificial intelligence can be defined as the software development technique that allows machines to work intelligently like humans, with the ability to be able to analyze and interpret a large amount of information to make future predictions in a short time with little effort [17] [18].

Artificial neural networks $(ANN)$ is a branch of artificial intelligence that simulates the human neural system to imitate human intelligent attitudes [18]. It consists in a system composed by several layers to analyze and provide answers to problems; these layers are divided into 3 main groups which are: input layer composed by a set of input neurons, hidden layer composed of one or more sets of hidden neurons and an output layer composed of a set of output neurons. The 3 layers are interconnected with each other, the neurons of the input layer send the data to the hidden layer which in turn transmit to the output layer [19]

### 2.3. The stress state

Underground rock formations are always under pressure, caused mainly by the overload of rocky materials and by tectonic origins. Any excavation change the pre-existing stress, it cause artificial disturbances and field stress redistribution [20].

Figure 1 illustrats a stress state in a volume element subject to a main field stress $\sigma_x$, $\sigma_y$ and $\sigma_z$ and its representation in cylindrical coordinates after a rotation $\theta$ using the equations 6, 7, 8 and 9 [21]:

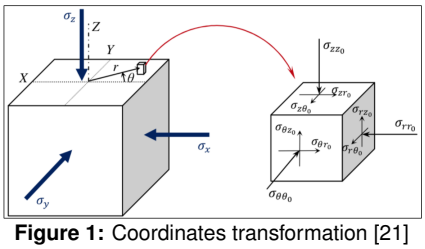

**Figure 1:** Coordinates transformation [21]

$$\sigma_{rr0} = \left(\frac{\sigma_x + \sigma_y}{2}\right) + \left(\frac{\sigma_x - \sigma_y}{2}\right)\cos 2\theta \quad (6)$$

$$\sigma_{\theta\theta 0} = \left(\frac{\sigma_x + \sigma_y}{2}\right) - \left(\frac{\sigma_x - \sigma_y}{2}\right)\cos 2\theta \quad (7)$$

$$\tau_{r\theta 0} = -\left(\frac{\sigma_x - \sigma_y}{2}\right)\sin 2\theta \quad (8)$$

$$\sigma_{zz0} = \sigma_z - \nu \times (\sigma_x + \sigma_y) \quad (9)$$

Where $\sigma_x$, $\sigma_y$ and $\sigma_z$ correspond the principal stresses in the cartesian plane; $\nu$, the poisson coefficient of the material, and $\sigma_{rr0}$, $\sigma_{\theta\theta 0}$, $\sigma_{zz0}$ and $\tau_{r\theta 0}$ the stresses in the cilindrical coordinates.

Induced stress around the excavation can be determined from the equations of Ernst Gustav Kirsch (1841–1901) [22]. The figure 2, shows the state of non-hydrostatic stress around a shaft with radius $a$; induced radial and tangential stresses at any point around an excavation can be determined according to the Kirsch equations below [22].

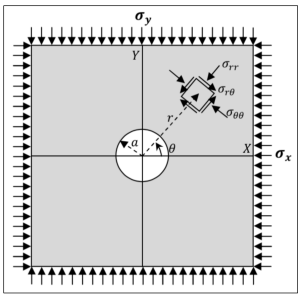

**Figure 2:** Stress arround the shaft [21]

$$\sigma_r = \frac{(\sigma_x + \sigma_y)}{2}\left(1 - \frac{a^2}{r^2}\right) + \frac{(\sigma_x - \sigma_y)}{2} \times \left(1 + \frac{3a^4}{r^4} - \frac{4a^2}{r^2}\right)\cos 2\theta \quad (10)$$

$$\sigma_\theta = \frac{(\sigma_x + \sigma_y)}{2}\left(1 + \frac{a^2}{r^2}\right) - \frac{(\sigma_x - \sigma_y)}{2} \times \left(1 + \frac{3a^4}{r^4}\right)\cos 2\theta \quad (11)$$

$$\sigma_z = \sigma_v - \nu\left[2\left(\sigma_x - \sigma_y\right)\frac{a^2}{r^2}\cos 2\theta\right] \quad (12)$$

$$\tau_{r\theta} = -\frac{(\sigma_x - \sigma_y)}{2}\left(1 - \frac{3a^4}{r^4} + \frac{2a^2}{r^2}\right) \quad (13)$$

$$\tau_{rz} = \tau_{\theta z} = 0 \tag{14}$$

Wherein $\sigma_r$ and $\sigma_\theta$ represent respectively radial and tangential stresses, $r$, distance to the center of the shaft, $a$, shaft radius, $\nu$, poisson coefficient, $\sigma_v$, vertical stress, $\sigma_x$ and $\sigma_y$ maximum and minimum horizontal stresses respectively, $\tau_{r\theta}$, $\tau_{rz}$ and $\tau_{\theta z}$, correspond to shear stresses in the respective directions $r\theta$, $\theta$, angle measured counterclockwise from direction of maximum stress ($\sigma_x$).

### 2.4. Shaft breakouts

Shaft breakouts are enlargements or enlargements of the shaft in a preferred direction, and are formed by fragments or spalling in a parallel direction to the minimum horizontal stress $(\sigma_{hmin})$ [23].

Shear and tensile failure are caused in the shaft by the action of the drilling mud as shown in the figure 3 [24]. Shear breakout occur when the shear stress along a plane reaches the shear strength of the rock, tensile breaks occur when the stresses exceed rock mass tensile strength[8].

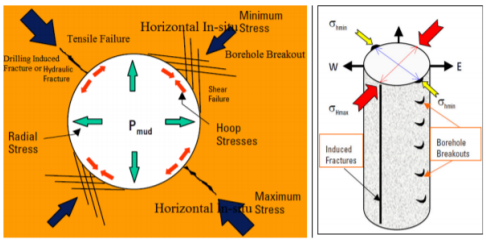


**Figure 3:** Borehole breakout[24]

According to the stress magnitude applied to the shaft walls, shear breakout can be classified as follows:

Wide breakout ($\sigma_\theta > \sigma_z > \sigma_r$) and narrow breakout ($\sigma_r > \sigma_z > \sigma_\theta$) occur in the radial and tangential plane since the maximum and minimum stresses are oriented in this plane.

High-angle echelon ($\sigma_z > \sigma_r > \sigma_\theta$) and low-angle echelon ($\sigma_\theta > \sigma_r > \sigma_z$) breakout occur in the axial and tangential plane since the maximum and minimum stresses are oriented in the arc of the shaft walls.

Shallow knockout ($\sigma_z > \sigma_\theta > \sigma_r$) and deep knockout ($\sigma_r > \sigma_\theta > \sigma_z$) breakout occur in the radial/ axial plane due to the orientation of the maximum and minimum stresses coinciding with this plane.

According to the stress magnitude around the shaft, the tensile strengths can be classified as follows [8]:

Cylindrical tensile breakout occur when $\sigma_r \leq -T_0$ creating concentric fractures with the shaft.

Horizontal tensile breakout occur when $\sigma_z \leq -T_0$ creating horizontal fractures.

Vertical tensile breakout occur when $\sigma_\theta \leq -T_0$ creating a vertical fracture in the parallel direction of the maximum principal stress.

## 3. Case study

The purpose of this subsection is to describe the methodology used to assess shaft stability.

Figure 4 summarizes the methodology followed to assess the shafts. The methodology comprises 5 fases, namely: shaft selection, collect data, rock mass classification, numerical modelling and result analysis.

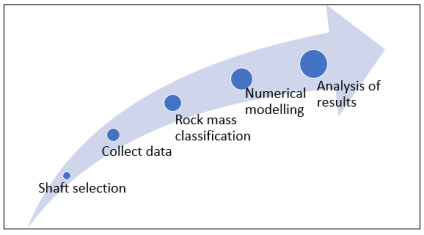


**Figure 4:** Methodology

Neves-Corvo has more than $500$ shafts, the first step was shaft selection. The shafts were selected according to the following criteria:

1. Ventilation shaft;
2. Evaluated with McCraken and Stacey method;
3. Shaft opened after 2013

Table 3 illustrate the shaft selected according to defined criteria.

**Table 3:** Chosen shafts to study

| Nº | Shaft | Depth(**m**) | Diameter(**m**) | Dip(**º**) | Length(**m**) |
|---|---|---|---|---|---|
| **1** | CV305 | 614 | 2,1 | 82,2 | 135 |
| **2** | CV338 | 610 | 2,1 | 89,2 | 120 |
| **3** | CV339 | 610 | 3,1 | 88,8 | 228 |
| **4** | CV359 | 610 | 3,1 | 88,3 | 220 |
| **5** | CV379 | 480 | 2,1 | 90,0 | 158 |
| **6** | CV702 | 285 | 3,1 | 90,0 | 340 |
| **7** | CV704 | 825 | 2,1 | 90,0 | 94 |
| **8** | CV715 | 825 | 3,1 | 90,0 | 112 |
| **9** | CV716 | 825 | 3,1 | 90,0 | 141 |
| **10** | CV264 | 480 | 2,1 | 84,9 | 96 |

The data used in this dissertation comes from the collection data in situ and provided by the company. To analyze the stress variation around the shaft, pre-existing field stress is calculated according to the gradient shown in the table 4

**Table 4:** Stress gradient [25]

| **Stress** | **Gradient**$(MPa/m)$ | **Trend**$(^\circ)$ | **Dip**$(^\circ)$ |
|---|---|---|---|
| $\sigma_1$ | 0,083 | 132 | 20 |
| $\sigma_2$ | 0,039 | 30 | 30 |
| $\sigma_3$ | 0,025 | 250 | 53 |

Neves-Corvo mine is composed by several lithologies, however they are grouped into $4$ main

types: shales, gradewaques, volcanic (cupriferous fissural) and massive sulfides [25]. The rocks have different geomechanical behaviors, according to data provided by the company the properties are illustrated in table 5.

**Table 5:** Rock Properties [25]

| Properties | Shales | Greywake | Volcanics | Massive Sulphide |
|---|---|---|---|---|
| Compressive strength, $\sigma_c$ (MPa) | 50 | 100 | 160 | 200 |
| Tensile strength, $\sigma_t$ (MPa) | 0,52 | 0,37 | 1,35 | 1,69 |
| Young module, $E$(GPa) | 30 | 42 | 60 | 87,5 |
| Density, $\gamma$ (Kg/m$^3$) | 3000 | 2800 | 3050 | 4500 |
| Poisson coefficient, $\nu$ | 0,32 | 0,28 | 0,14 | 0,14 |
| Friction angle, $\phi(°)$ | 32,4 | 41,6 | 48,5 | 50,1 |
| Cohesio, $c$ (MPa) | 4.66 | 6,31 | 9,52 | 10,64 |

The data from the tables 4 and 5, are inputs in $RS^3$ software numerical modeling.

Considering the criteria defined for shaft selection in section 3, geotechnical logs were made from the surveys, data collection on company database, and observations of in situ conditions. After collecting, processing and analyzing the data, $MS$ classifications and modeling were applied.

Table 6 illustrate the field stress on top of the shaft before excavation according to the stress gradient and depth.

**Table 6:** Field stress on top of the shaft before excavation

| Nº | Shaft | Depth(m) | $\sigma_1$(MPa) | $\sigma_2$(MPa) | $\sigma_3$(MPa) |
|---|---|---|---|---|---|
| **1** | CV305 | 614 | 51 | 23 | 15 |
| **2** | CV338 | 610 | 51 | 23 | 15 |
| **3** | CV339 | 610 | 51 | 23 | 15 |
| **4** | CV359 | 610 | 51 | 23 | 15 |
| **5** | CV379 | 480 | 40 | 18 | 12 |
| **6** | CV702 | 285 | 24 | 11 | 7 |
| **7** | CV704 | 825 | 68 | 31 | 21 |
| **8** | CV715 | 825 | 68 | 31 | 21 |
| **9** | CV716 | 825 | 68 | 31 | 21 |
| **10** | CV264 | 480 | 40 | 18 | 12 |

## 4. Results

The results obtained from the methods used are presented and discussed in this section, specifically $MS$ method, numerical modelling $(RS^3)$ and comparative results with in situ classification.

### 4.1. Rock mass classification

Based on McCraken and Stacey method from collected data, tables 7 and 8 present the quantitative and qualitative classification.

**Table 7:** Shaft quantitative classification

| Nº | Shaft | RQD | $Q_r$ | Diameter(m) | Span(m) |
|---|---|---|---|---|---|
| **1** | CV305 | 64 | 1,94 | 2,1 | 3,39 |
| **2** | CV338 | 54 | 0,87 | 2,1 | 2,46 |
| **3** | CV339 | 69 | 2,64 | 3,1 | 3,83 |
| **4** | CV359 | 43 | 0,1 | 3,1 | 1,04 |
| **5** | CV379 | 94 | 1,88 | 2,1 | 3,35 |
| **6** | CV702 | 53 | 2,21 | 3,1 | 3,57 |
| **7** | CV704 | 89 | 3,43 | 2,1 | 4,26 |
| **8** | CV715 | 96 | 5,42 | 3,1 | 5,11 |
| **9** | CV716 | 81 | 1,38 | 3,1 | 2,96 |
| **10** | CV264 | 53 | 0,99 | 2,1 | 2,59 |

According to table 7 analysis, it was verified that shafts have $RQD$ classification higher than $50\%$ except CV359. It's also possible to identify that the $span_{max}$ is larger than the diameter for major shafts, except for the CV359 and the CV716 despite its high $RQD$

In order to make the analysis clear and simple, the qualitative classification of the rock mass is present on table 8 based on achieved results presented in table 7. According to McCracken and Stacey classification, shaft is stable if the maximum span is greater than its diameter $span_{max} \geq diameter)$, and otherwise is unstable.

**Table 8:** Shaft qualitative classification

| Nº | Shaft | RQD | Qr | Span max |
|---|---|---|---|---|
| 1 | CV305 | Fair | Poor | Stable |
| 2 | CV338 | Fair | Very Poor | Stable |
| 3 | CV339 | Fair | Poor | Stable |
| 4 | CV359 | Poor | Very Poor | Unstable |
| 5 | CV379 | Excellent | Poor | Stable |
| 6 | CV702 | Fair | Poor | Stable |
| 7 | CV704 | Good | Poor | Stable |
| 8 | CV715 | Excellent | Fair | Stable |
| 9 | CV716 | Good | Poor | Unstable |
| 10 | CV264 | Fair | Very Poor | Stable |

By analyzing the results of table 8 it's possible to verify according to $MS$ method mostly shaft presents a stable classification for opening with the diameter of each shaft indicated in the table 7, with the exception of CV359 and CV716 that represent $20\%$ unstable. Despite the stable classification, some of these shafts was identified instability problems.

### 4.2. Shaft analysis

To analyze the shaft stability using numerical modeling, three parameters were used to assist in the characterization of the field stress and rock mass stability, namely, the main stresses $\sigma_1$ and $\sigma_3$, and safety factor.

The results presented bellow correspond to CV305, just for example to illustrate the methodology, however, the final result of each shaft can be found in table 9

Figures 5 and 6 illustrate respectively the $\sigma_1$ and $\sigma_3$ distribution around shaft. In figure 5 the high maximum principal stress, $\sigma_1$, concentrate in direction of the minimum horizontal stress $(\sigma_{h_0min})$ $(N40E)$ around $102MPa$, and a lower concentration is slightly perpendicular in direction $(\sigma_{h_0max})$ around $N130E$.

Figure 6 illustrate the minimum principal distribuition around de shaft $(\sigma_3)$ with the high stress distribuition in direction of the minimum horizontal stress $(\sigma_{h_0min})$ $(N40E)$ around $20MPa$, and a lower concentration in the slightly perpendicular direction $(\sigma_{h_0max})$ $(N130E)$.

The maximum and minimum principal stress $(\sigma_1)$ $(\sigma_3)$ correspond to stresses $\sigma_\theta$ and $\sigma_r$ respectively. Since $\sigma_\theta > \sigma_z > \sigma_r$ the probable breakout in this

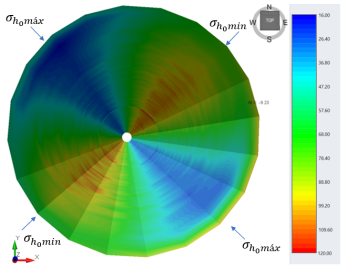


**Figure 5:** $\sigma_1$ of CV305

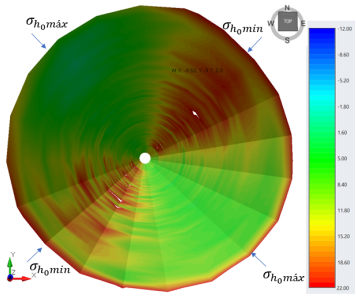


**Figure 6:** $\sigma_3$ of CV305

shaft will be wide breakout also known as dog ear.

The figure 7 illustrate the safety factor $SF$ variation around CV305. It is worth knowing that this parameter depends not only on the stress applied but also on the rock mass properties. $SF$ is a relevant parameter in the stability assessment, as it allows identify potentially stable and unstable zones.

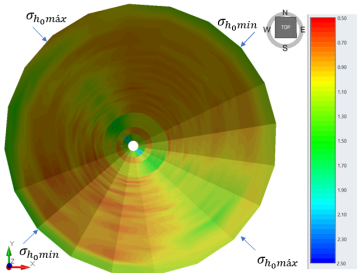


**Figure 7:** CV305 safety factor

Potentially unstable zones correspond to $SF < 1$, and if not, correspond to stable zones. In the models generally speaking, potentially stable zone is located essentially in the direction ($\approx 140°$) which corresponds to the orientation of the maximum horizontal stress $(\sigma_{h_0max})$.

On the other hand, it is possible to identify $SF$ variation along the shaft according to different lithologies that the shaft through. The potentially stable zone is mostly found in the last $50m$ due to the rock type existing in this range.

For quantitative analysis $27$ points with approximately $5m$ spacing along the shaft in the critical direction $(\sigma_{h_0min})$ was chosen to analize with more detail. Figure 8$(a)$ illustrate the safety factor log resulted in the model, where two potentially undesirable zones can be identified with an approximate $45m$ length, which represents just over $30\%$ of its total length. According to unstable zones identified along CV305 has an overall safety factor of $FS = 0.91$ (table 9), so it is classified globally as potentially unstable.

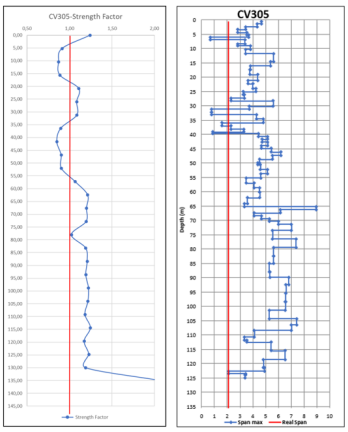


**Figure 8:** CV305-Shaft log

On the other hand, figure beside 8 $(b)$ illustrate the CV305 geotechnical profile resulting from MS method application. By analyzing the figure, it is possible to identify $3$ pontencially unstable zones $(span_{max} < diameter)$ that represent almost $10\%$ of shaft's total length. CV305 has a $span_{max} = 3.39$ (table 7) and a diameter of $2.1m$. For this reason, it is classified as globally stable according to MS method.

### 4.3. Summary Results

Table 9 summarizes the achieved results of numerical modelling on critical direction $(\sigma_{h_0min})$ along the shaft to consider the worst case scenario. In table 9, safety factor and principal stress of each shaft correspond to percentile $20$ and $80$ respectivelly.

For the same depth has similar stress after excavation ($2°$ stage) owing to the field stress applied in the model is the same (6).

**Table 9:** Summary results from critical direction $(\sigma_{h_0min})$

| Nº | Shaft | Depth(m) | $\sigma_1$(MPa) | $\sigma_3$(MPa) | SF |
|---|---|---|---|---|---|
| **1** | CV305 | 614 | 102 | 20 | $0,91$ |
| **2** | CV338 | 610 | 99 | 18 | $0,93$ |
| **3** | CV339 | 610 | 98 | 17 | $0,91$ |
| **4** | CV359 | 610 | 95 | 17 | $0,86$ |
| **5** | CV379 | 480 | 75 | 12 | $1,20$ |
| **6** | CV702 | 285 | 46 | 9 | $0,98$ |
| **7** | CV704 | 825 | 132 | 26 | $1,04$ |
| **8** | CV715 | 825 | 132 | 25 | $1,04$ |
| **9** | CV716 | 825 | 130 | 21 | $1,08$ |
| **10** | CV264 | 480 | 77 | 15 | $1,10$ |

Analyzing the table 9 results, safety factor is a parameter with low amplitude, however shaft at $600m$ depth are classified as potentially unstable $(FS < 1)$ , in general this classification is not observed in shaft at greater or lower depths than

$600m$, so it is associated with the lithology in this region. It can also be seen that the stresses $\sigma_1$ and $\sigma_3$ are similar in shaft at the same depth due to the stress gradient applied to the model.

Figure 9 illustrate MS classification method results, and only two shaft are classified as potentially unstable $span_{max} < diameter$.

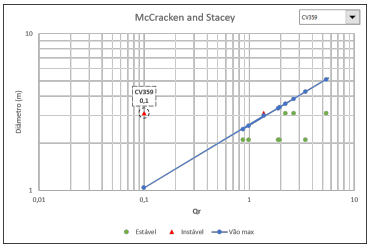


**Figure 9:** McCraken and Stacey stability classification

Figure 10 illustrate the global classification resulting from the numerical models, as it's possible to that $50\%$ of the shafts are classified as potentially unstable owing to $FS < 1$.

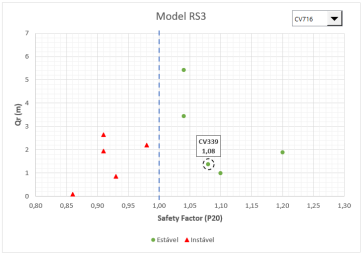


**Figure 10:** Shaft classification according to the model

Based on achieved results, table 10 illustrate qualitative results from numerical modelling $(RS^3)$, MS and in situ classification.

**Table 10:** Achieved results

| Nº | Shaft | SF | Model Classification | MS Classification | Real Classification |
|---|---|---|---|---|---|
| 1 | CV305 | 0,91 | Unstable | Stable | Unstable |
| 2 | CV338 | 0,93 | Unstable | Stable | Unstable |
| 3 | CV339 | 0,91 | Unstable | Stable | Unstable |
| 4 | CV359 | 0,86 | Unstable | Unstable | Unstable |
| 5 | CV379 | 1,20 | Stable | Stable | Stable |
| 6 | CV702 | 0,98 | Unstable | Stable | Stable |
| 7 | CV704 | 1,04 | Stable | Stable | Stable |
| 8 | CV715 | 1,04 | Stable | Stable | Stable |
| 9 | CV716 | 1,08 | Stable | Unstable | Stable |
| 10 | CV264 | 1,10 | Stable | Stable | Stable |

Results obtained in the models correspond $90\%$ of in situ classification, whereas $MS$ method correspond $60\%$ of the studied cases, this difference among the results obtained is justified by the fact that the numerical model contemplates the alteration of the field stress in greater detail, whereas $MS$ uses the geomechanical classifications.

CV702 is classified as unstable according to the model, however, it is stable on in situ classification observed to date. Based on the results, it is worth noting that the model is conservative because classify as unstable, and although there are currently no instability problems, it does not mean that it cannot occur over time. Shaft CV702 was opened relatively recently $(2018)$, and has a safety factor $SF = 0.98$ close to the stability limit.

## 5. Conclusions

### 5.1. Conclusions

Based on the achieved results in this study, shaft assessment with numerical simulations and McCracken and Stacey classification, the following considerations are made.

During the shaft opening phase, drilling deviations may occur depending on the lithologies dip, speed drilling for any type of rock mass.

The field stress distribution around the shaft at the same depth, is very similar in the models due to the initial stress applied, with a greater concentration in direction of maximum principal stress $\sigma_{h_0min}$, $(\approx N40E)$ and a stress relief in the perpendicular direction to the horizontal plane that corresponds to the direction $\sigma_{h_0máx}$. However, the shaft size, the orientation and lithologies types generate different safety factors.

For Neves-Corvo Mine field stress, the maximum $(\sigma_1)$ and minimum $(\sigma_3)$ principal stress correspond to tangential, $\sigma_\theta$, and radial stresses, $\sigma_r$, respectively, in sub-vertical circular excavations, and $\sigma_\theta > \sigma_z > \sigma_r$, therefore, the breakout likely to occur after excavation due to the field stress is wide breakout also known as dog ear.

Regarding the safety factor, instability was observed in the direction of $\sigma_{h_0min}$, in $5$ ventilation shaft, which represents $50\%$ of the cases studied. In the in situ classification (by observation on the ground) $4$ shaft were identified as unstable, thus the classification of the models correspond $90\%$ reality. As for the MS classification, it only correspond $60\%$ reality, with $2$ unstable and $8$ stable.Although results obtained in the model and the MS method correspond to $90\%$ and $60\%$ of reality, respectively, so we recommends to use both methods.


### 5.2. Acknowledgement

First of all, I want to thank God for everything, and secondly, my supervisor Prof.ª Maria Matilde Costa e Silva for all support along the course, and a special thanks goes to Eng.º João Gabriel and Eng.ª Erminia Marras for shared their experience.


### References


[1] General Kinematics, "A BRIEF HISTORY OF MINING: THE ADVANCEMENT OF MINING TECHNIQUES AND TECHNOLOGY," 2019 (accessed $17^{th}$/06/2019).

[2] S. M. Aminossadati and K. Hooman, "Numerical Simulation of Ventilation Air Flow in Underground Mine Workings," *12th US/North American Mine Ventilation Symposium*, no. 1974, pp. 253–260, 2008.

[3] J. Tien, “Mine Ventilation Systems,” no. 1, pp. 162–183, 1999.

[4] W. A. Hustrulid, J. L. Mero, and G. B. Clark, “Mining,” 2017.

[5] A. McCracken and T. R. Stacey, “Geotechnical risk assessment for large-diameter raisebored shafts,” in *Tunnelling ’88: Papers Presented at the Fifth International Symposium*, (London), Institution of Mining and Metallurgy, 1988.

[6] R. Lyle, “Considerations for large-diameter raiseboring,” in *Proceedings of the First International Conference on Underground Mining Technology* (M. Hudyma and Y. Potvin, eds.), pp. 581–595, Australian Centre for Geomechanics, 2017.

[7] E. Hoek, “Pratical Rock Engineering,” 2007.

[8] B. Pašić, N. Gaurina-Medimurec, and D. Matanović, “Wellbore instability: Causes and consequences,” *Rudarsko Geolosko Naftni Zbornik*, vol. 19, pp. 87–98, 2007.

[9] M. N. Bidgoli, Z. Zhao, and L. Jing, “Numerical evaluation of strength and deformability of fractured rocks,” *Journal of Rock Mechanics and Geotechnical Engineering*, vol. 5, no. 6, pp. 419–430, 2013.

[10] A. Swart, T. Stacey, J. Wesseloo, W. Joughin, K. Roux, D. Walker, and R. Butcher, “Investigation of factors governing the stability/instability of stope panels in order to define a suitable design methodology for near surface and shallow mining operations,” Tech. Rep. July, 2000.

[11] D. W. D. U. D. Deere, “The rock quality designation (RQD) index in practice,” 1988.

[12] N. R. Barton, R. Lien, and Lunde J., “Engineering Classification of Rock Masses for the Design of Tunnel Support,” *Rock Mechanics*, vol. 6, pp. 189–236, December 1974.

[13] S. Panthee, P. K. Singh, A. Kainthola, and T. N. Singh, “Control of rock joint parameters on deformation of tunnel opening,” *Journal of Rock Mechanics and Geotechnical Engineering*, vol. 8, no. 4, pp. 489–498, 2016.

[14] S. Bock, “Numerical Modelling of a Void Behind Shaft Lining using FDM with a Concrete Spalling Algorithm,” *Journal of Sustainable Mining*, vol. 13, no. 2, pp. 14–21, 2014.

[15] Rocscience, “Products for excavation design.” https://www.rocscience.com/software/excavation-design, 2019 (accessed $3^{rd}$/5/2019).

[16] T. Miranda, A. Correia, I. Nogueira, M. Santos, P. Cortez, and L. Sousa, “Alternative models for the calculation of the rmr and q indexes for granite rock masses,” pp. 151–162, 03 2007.

[17] J. McCarthy, “What Is Artificial Intelligence?,” 2007.

[18] I. Gomaa, S. Elkatatny, and A. Abdulraheem, “Real-time determination of rheological properties of high over-balanced drilling fluid used for drilling ultra-deep gas wells using artificial neural network,” *Journal of Natural Gas Science and Engineering*, vol. 77, no. February, p. 103224, 2020.

[19] H. Zhang, H. Nguyen, X. N. Bui, T. Nguyen-Thoi, T. T. Bui, N. Nguyen, D. A. Vu, V. Mahesh, and H. Moayedi, “Developing a novel artificial intelligence model to estimate the capital cost of mining projects using deep neural network-based ant colony optimization algorithm,” *Resources Policy*, vol. 66, no. October 2019, p. 101604, 2020.

[20] S. S. M. Chan and M. J. Beus, “Structural Design Considerations for Deep Mine Shafts.,” *Report of Investigations - United States, Bureau of Mines*, 1985.

[21] A. Mirahmadizoghi, “Analysis of Rock Performance under Three-Dimensional Stress to Predict Instability in Deep Boreholes, Ph.D. Thesis,” no. September, 2012.

[22] B. H. G. Brady and E. T. Brown, *Rock Mechanics*, vol. 34. 2004.

[23] S. Prensky, “Borehole Breakouts and In-situ Rock Stress–A Review,” *The Log Analyst*, vol. 33, no. 3, pp. 304–312, 1992.

[24] M. Alizadeh, Z. Movahed, R. Junin, R. Mohsin, M. Alizadeh, and M. Alizadeh, “Finding the Drilling Induced Fractures and Borehole Breakout Directions Using Image Logs Akademia Baru,” *Journal of Advanced Research in Applied Mechanics*, vol. 10, no. 1, pp. 9–29, 2015.

[25] Departamento de Mecânica da Rocha, *Fundamentos e Regras Básicas da Mecânica das Rochas*, vol. II. Castro Verde, Beja, Portugal: SOCIEDADE MINEIRA DE NEVES-CORVO, 2010.